

# Study on Heat Transfer Characteristics during Solidification of 18-ton Steel Ingot with Large Ratio of Height to Diameter

Z. Yu, H. Zhang, X. Wang, X. Wu

In order to investigate the heat transfer characteristics during solidification of steel ingot with large ratio of height to diameter, numerical simulations of solidification process of 18-ton steel ingot were carried out. The simulated results were verified by the temperatures measurement during solidification of steel ingot. In addition, in order to further certify the mathematical model, the solidification process of 5.3-ton ingot has been investigated, the simulated shape and length of the shrinkage pipe of steel ingot agree well with the experimental result observed by the sectioning. It is found that the heat of molten steel is mainly transferred to the external environment through ingot body. With this context, the analytical method using the concept of thermal resistance is proposed to explore the heat transfer resistances of outer wall of mold, mold, ingot/mold interface and solidified shell. Consequently, the transient thermal resistances at different stages of steel ingot solidification were dug out. Based on the analyses of the heat transfer resistances at different stages of steel ingot solidification with different casting parameters, it is obtained that heat transfer of solidified shell is the main restrictive step of heat transfer in the whole solidification process for 18-ton steel ingot with large ratio of height to diameter.

**KEYWORDS:** KEYWORDS SOLIDIFICATION, STEEL INGOT, HEAT TRANSFER CONTROL, THERMAL RESISTANCE, NUMERICAL SIMULATION

## Introduction

Large steel ingots are the basic raw materials for the equipment manufacturing industry. Its production capacity is directly related to the national industrial development level and economic lifeline. The steel ingot solidification process has an important influence on its quality and the property of final product. The solidification rate of steel ingot depends on the heat transfer from molten steel to external environment. As is known to all, it is difficult to measure heat transfer parameters directly during solidification of a steel ingot. However, with the rapid development of computer technology, numerical simulation is being increasingly applied to study of solidification of steel ingot [1]-[4]. The author [5] developed a two-dimensional numerical model of ingot solidification, and temperature distribution, distribution solid and liquid phase were calculated. Zhang et al. [6] studied the effect of casting pro-

**Zhanyang Yu, Hui Zhang, Xuebing Wang**  
Central Iron and Steel Research Institute, Beijing 100081, China

**Xuan Wu**  
University of Science and Technology Beijing, Beijing 100083, China

cess parameters on the shrinkage of ingot by numerical method. Wang [7] et al. studied that the best criterion has

been found to be the condition under

$$G/R_s^{0.5} < 2.5^\circ\text{C s}^{0.5} \text{ mm}^{-1.5} \quad (o)$$

(G and  $R_s$  are the temperature gradient and solidification rate, respectively), with this criterion, the distribution and size of the simulated centerline shrinkage porosity agree well with the experimental results observed by the sectioning and ultrasonic testing. Since Flemings and co-workers published their pioneer papers on macrosegregation [8]-[11], the mathematical model of macrosegregation has been developed continuously. Li et al. [12][13] developed various models to study the formation of macrosegregation in ingots. Tu et al. [14] used a multicomponent multiphase model to study macrosegregation of 36-ton steel ingot. M. Wu et al. [15] introduced a four-phase mixed columnar-equiaxed solidification model to calculate the formation of shrinkage cavity and macrosegregation during solidification of steel ingot. So far, scholars have focused their research efforts on the formation of defects in ingots, such as shrinkage and macrosegregation. However, there are few reports on heat transfer control during solidification of ingots with large ratio of height to diameter.

In this paper, through FEM (Finite Element Method) simulation in combination with the temperature measurement and experimental sectioning investigation, the solidification process of 18-ton steel ingot with a large ratio of height to diameter were carried out. An important result is obtained from the analysis of heat transfer characteristics of ingot solidification, the heat of molten steel is mainly transferred to the external environment through ingot body. With this context, the heat transfer restriction steps of 18-ton ingot at different solidification stages were investigated.

In addition, the effects of increasing the cooling intensity of the outer wall of the mold and the variation of pouring temperature on the thermal resistances in different stages of solidification process of steel ingot were further dug out.

## Numerical Simulation of Solidification of 18-ton Steel Ingot

### Establishment of Mathematical Model

#### Governing equation and geometry model

The solidification process of steel ingot was investigated by finite element method in ProCAST package. Assumptions were made: (1) the temperature and velocity of the molten steel poured into the mold from the top have an even distribution; (2) the liquid metal was incompressible Newton fluid; (3) the convection was driven by thermal buoyancy; (4) the solutal convection was ignored; (5) the heat transfer was coupled with the mold filling. A three-dimensional model is established based on the governing equation, including the Navier–Stokes equation, the continuity equation, energy equation,  $\kappa$ - $\varepsilon$  equation, and VOF function.

The geometries and finite element mesh of the steel ingot, the mold, the insulation brick and bottom pad are shown in Figure 1. The finite element mesh of the mold, the ingot, the insulation brick and bottom pad consisted of 71512 nodes and 334535 tetrahedral elements, which were selected based on several mesh refinements.

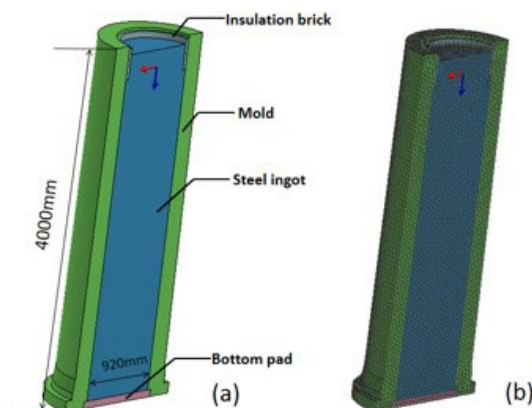


**Fig.1** - Geometric models and finite element mesh of the mold, steel ingot, insulation brick and bottom pad, (a) Geometric models, (b) finite element mesh

**Thermophysical parameters**

The thermophysical parameters of the Bottom Pad and

Insulation Brick are provided by the manufacturer, the values are shown in Table 1.

**Tab.1** - The thermophysical parameters of Bottom Pad and Insulation Brick

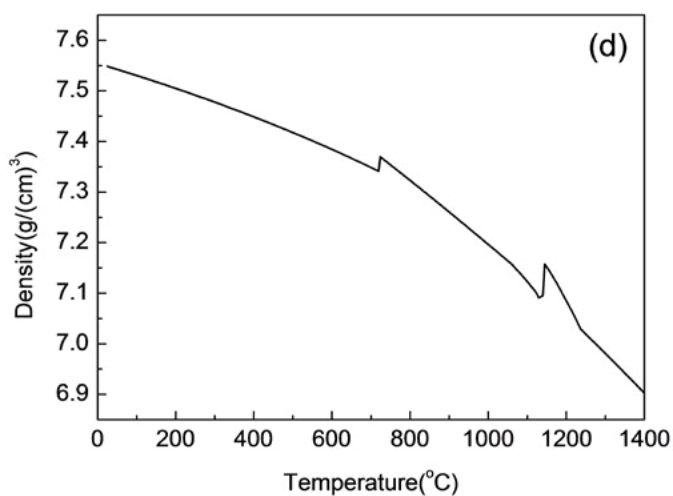
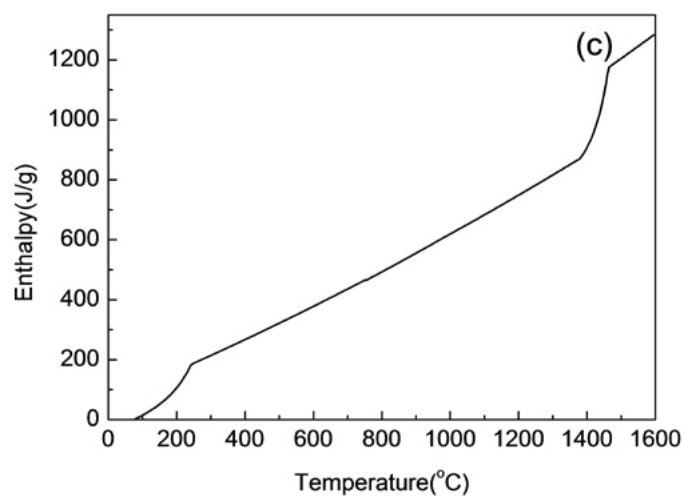
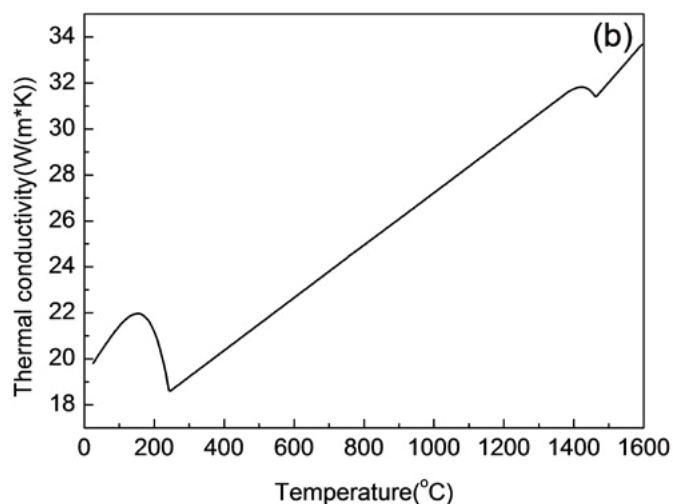
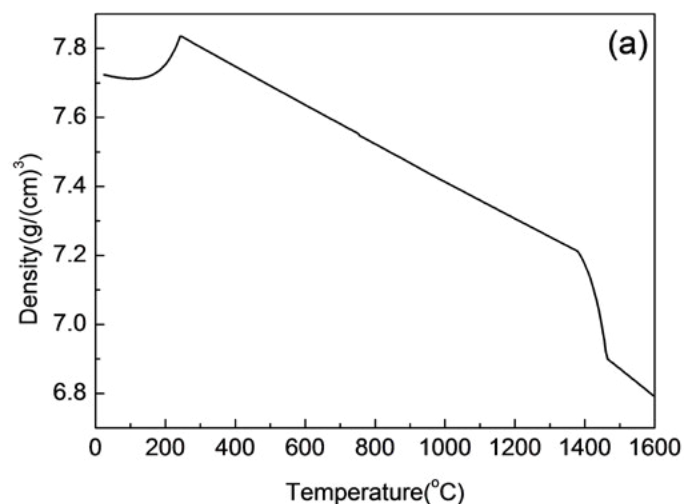
Material	Density(kg/m <sup>3</sup> )	Specific heat(J/gK)	Conductivity(W/(mK))
Bottom Pad	2900	1.5	4
Insulation Brick	500	1.08	0.78

The compositions of the steel ingot and mold are shown in Table 2. The thermophysical parameters of steel ingot

and mold are calculated via database system in ProCAST software, as shown in Figure 2.

**Tab.2** - Composition of the ingot and mold(wt.%)

Material	C	Si	Mn	P	S	Cr	Ni
Ingot	0.38-0.41	1.59-1.63	1.69-1.71	<0.005	<0.002	0.82-0.84	1.84-1.86
Mold (Ductile iron)	3.2-3.5	—	0.8-1.2	<0.005	<0.005	—	—



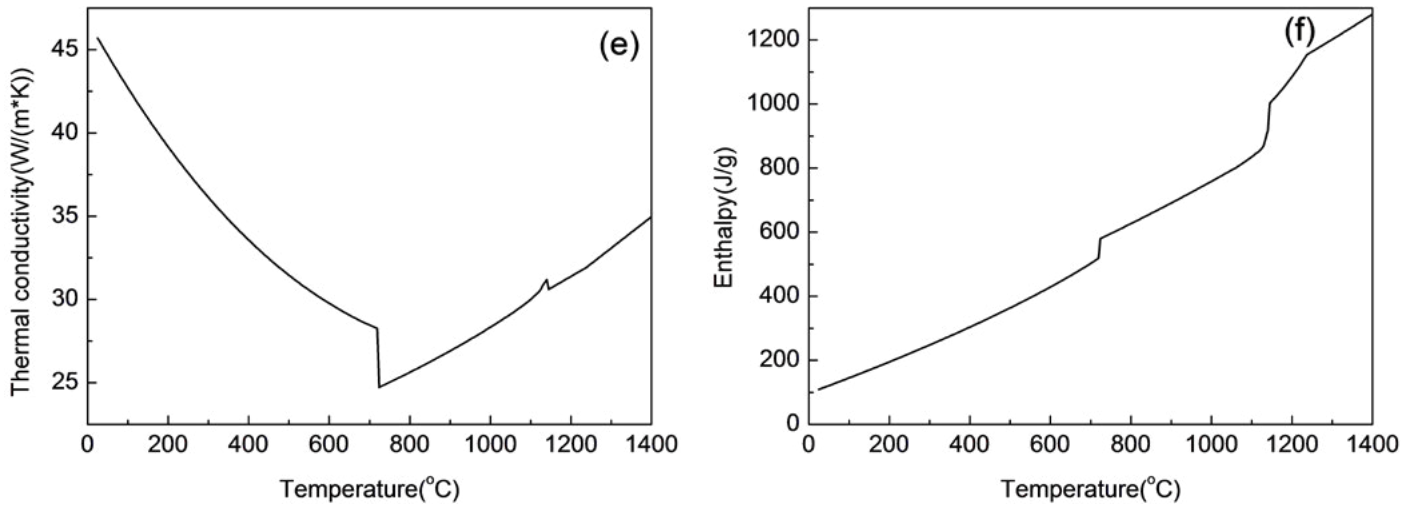


**Fig.2** - Physical parameters of the ingot and mold:(a) density of the ingot;(b) thermal conductivity of the ingot;(c) enthalpy of the ingot;(d) density of the mold;(e) thermal conductivity of the mold;(f) enthalpy of the mold.

**Boundary and initial conditions**

Because of the gap between ingot and mold, the heat

transfer coefficient of metal-mold interface changes with time[16][17].It is shown in equation 1.

$$h_{int} = \max(h_c, \sigma \epsilon_{eff} (T_{ii}^2 + T_{mi}^2) (T_{ii} + T_{mi})) \quad (1)$$

where  $h_c = 800(1-t/t_{gap})$ , and  $t_{gap}$  is average formation time of the gap between the ingot and mold;  $\epsilon_{eff}$  is effective emissivity in ingot/mold interface,0.7; $\sigma$  is Stefan–Boltzman constant,  $5.67 \times 10^{-8} \text{ W} \cdot \text{m}^{-2} \cdot \text{K}^{-4}$ ;  $T_i$  is temperature of the mold in ingot/mold interface,  $T_{mi}$  is temperature of the ingot in ingot/mold interface ;  $t_{gap}$  of 18 and 5.3 ton steel ingots were assigned as 1200s and 80s[18].

The heat transfer coefficients of both mold-insulation brick and steel-insulation brick interfaces were assigned as

$20 \text{ W} \cdot \text{m}^{-2} \cdot \text{K}^{-1}$ . The heat transfer coefficient between steel and bottom pad was assigned as  $100 \text{ W} \cdot \text{m}^{-2} \cdot \text{K}^{-1}$ .The heat transfer coefficient between mold and bottom pad was assigned as 200 ;The heat transfer coefficient between base and bottom pad was assigned as 100 .

The heat transfer coefficient of the outer wall of mold wall was assigned according to the following Equation 2 in which both radiation and convection heat transfer were taken into consideration[19].

$$h_{ext} = \sigma \epsilon_{me} (T_{me}^2 + T_{\infty}^2) (T_{me} + T_{\infty}) + 1.24 (T_{me} - T_{\infty})^{0.33} \quad (2)$$

where  $T_{me}$  is the temperature around mold wall;  $T_{\infty}$  is the equivalent temperature of surroundings;  $\epsilon_{me}$  is emissivity of outer wall of the mold,0.85; and  $\sigma$  is the Boltzmann constant.

The heat transfer between the top of the ingot and the external environment is also treated according to equation 2. The initial values for each material are shown in Table 3.

**Tab.3** - Initial temperature values for each material

Material	Steel	Mold	Insulation brick	Bottom pad
Initial value/°C	1560	80	40	200

**Verification of Mathematical Model**

**Verification of temperature**

In order to verify the accuracy of numerical simulation of ingot solidification, industrial experiments were carried out in a steel plant. The temperature change of the outer wall of

the mold during solidification of ingot was measured. Comparison between calculated results and measured values are shown in Figure 3. As can be seen that the calculated values agree well with the measured ones.

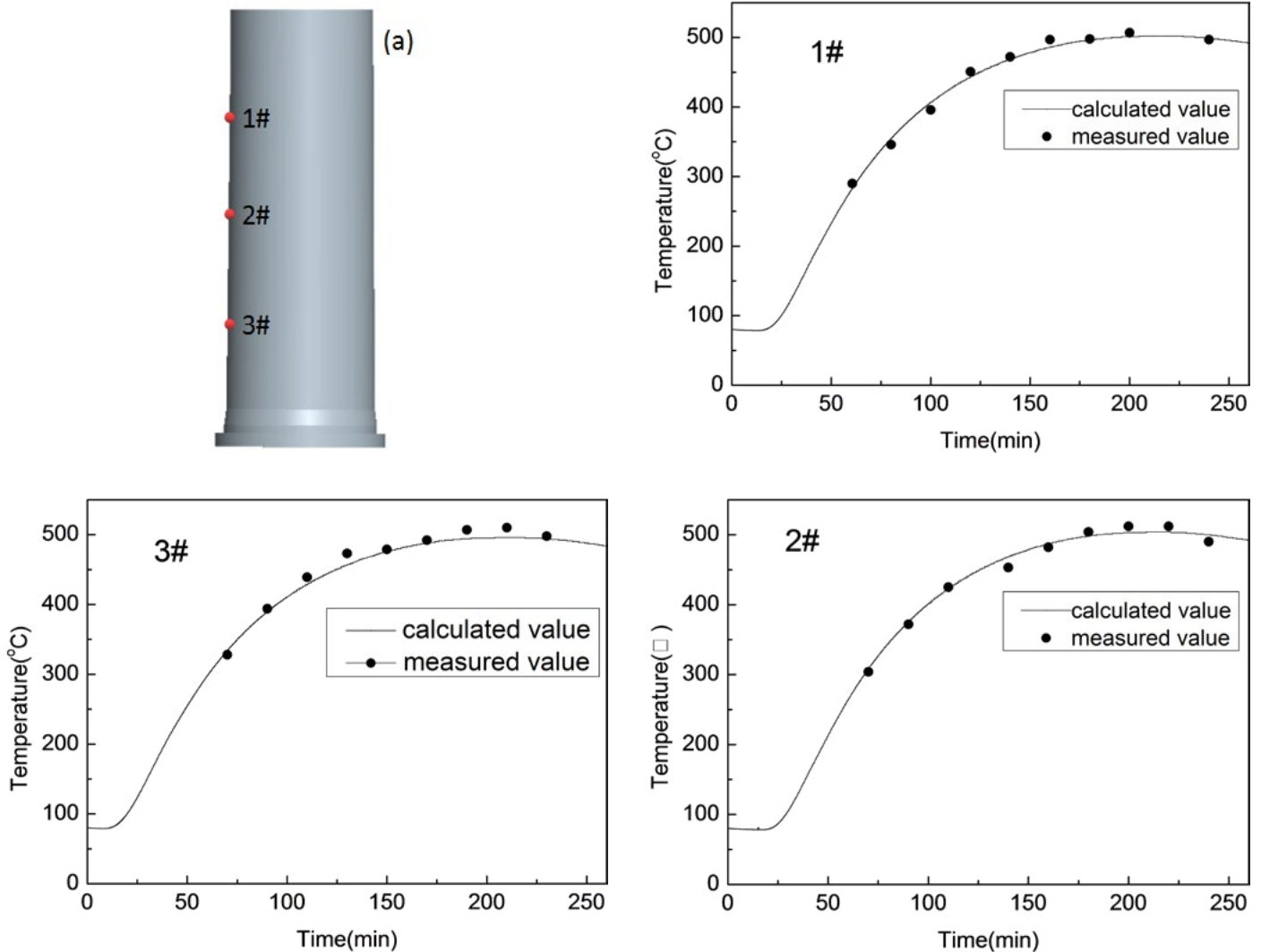


**Fig.3** - Position of measured point and comparison of calculated temperature with measured ones,(a) position of measured point,1#, 2# and 3# are the number of measuring points

**Verification of shrinkage pipe**

In order to further certify the mathematical model, the solidification process of 5.3-ton ingot with a height of 2820 mm and a diameter of 590 mm has been investigated. Figure 4 compiles the sectioned surface at top of the ingot (panel

(A)), photo of the 5.3-ton ingot (panel(B)), calculated result (panel(C)), respectively. Figure 4 (A) and (C) confirmed that the simulated shape and length of the shrinkage pipe of the ingot are in good agreement with the experimental result observed by the sectioning.

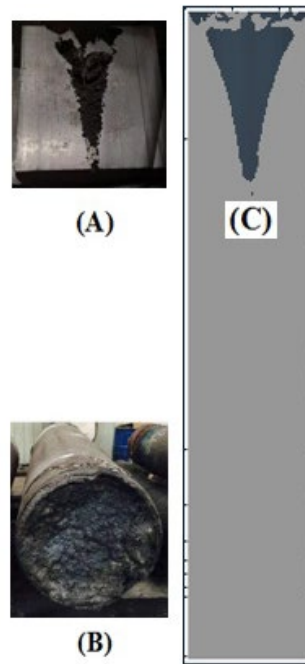


**Fig.4** - The sectioned surface at top of the ingot (A), photo of the 5.3-ton ingot (B), calculated result (C)

Consequently, through FEM (Finite Element Method) simulation in combination with the temperature measurement and experimental sectioning investigation of the ingot, it is concluded that the mathematical model of solidification process of ingot with large ratio of height to diameter in this paper is quite accurate.

## Results and Discussion

### Heat Transfer Characteristics of Steel Ingot Solidification

Fraction solid distribution at different time during ingot solidification is shown in Figure 5. As can be seen from figure that after the mold is filled with molten steel, the solidifica-

tion front moves to the center of the ingot in a "deep U" shape. The reason for this phenomenon is that the solidification rate of ingot body is faster than that of top and bottom of ingot. In the final stage of solidification of the steel ingot, the liquid steel in the center of ingot can solidify simultaneously and can't be supplemented by the surrounding liquid metal, which easily leads to the defect formation of the shrinkage porosity. At the end of ingot solidification, a deep shrinkage pipe was formed at the top of the ingot, which is one of the characteristics of solidification of steel ingot with large ratio of height to diameter.

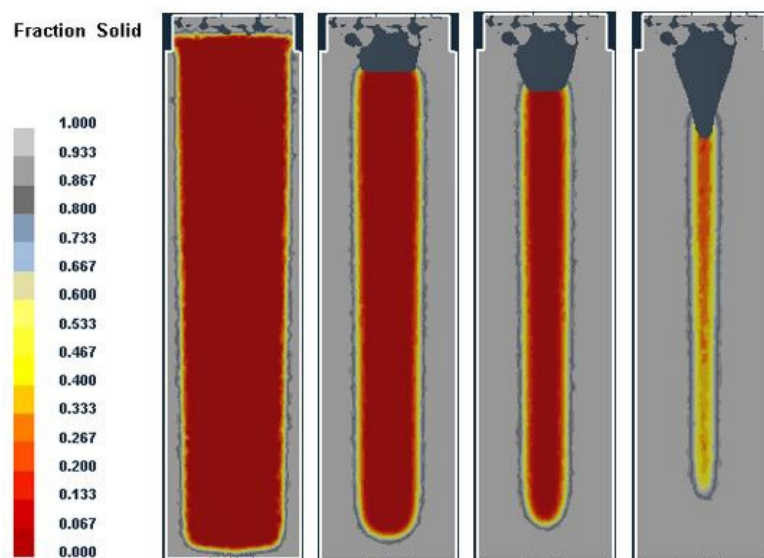


**Fig.5**- Fraction solid distribution at different time during ingot solidification

Figure 6 shows evolution of heat storage of the mold during solidification, as can be seen from figure that in the early stage of solidification, the heat storage of mold is almost equal to the heat through the inner wall of mold. With the development of solidification, the temperature on the outer wall of the mold is much higher, which accelerates the efficiency of heat transfer from the outer wall of the mold to the environ-

ment, which leads to that the heat storage of mold increases slowly in the middle and late stages of solidification. Consequently, the mold is always in the state of heat storage during the whole solidification process of ingot, which is another characteristic of solidification of steel ingot with large ratio of height to diameter.

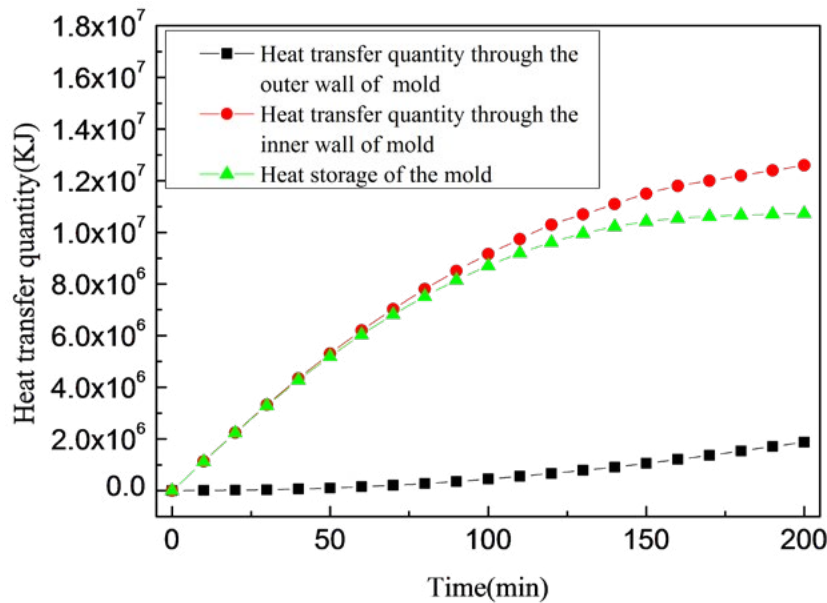


**Fig.6** - Evolution of heat storage of the mold during solidification

During the ingot solidification, the superheat and latent heat of molten steel are transferred to the external environment through those paths: 1) top of the ingot; 2) the side of the insulation brick; 3) ingot body; 4) bottom of the ingot, as shown in Figure 7 (A). Proportion of total heat transfer quantity at dif-

ferent parts of ingot at the end of solidification is shown in Figure 7(B). As can be seen that the heat of molten steel is mainly transferred to the external environment through ingot body.

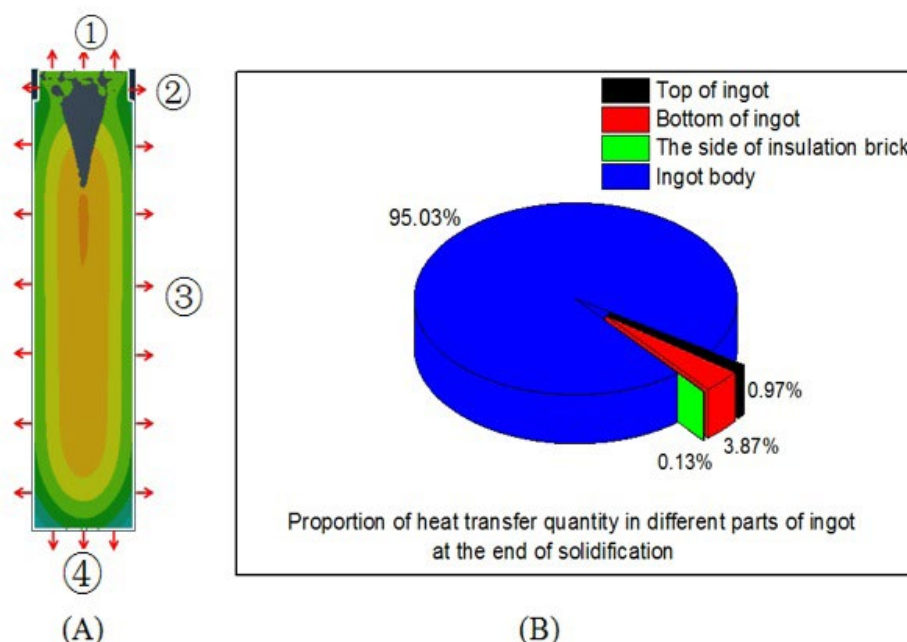


**Fig.7** - Proportion of total heat transfer quantity at different parts of ingot at the end of solidification

### Thermal Resistance

The result is obtained from Figure 7 (B), during the solidification process of ingot, the superheat and latent heat of molten steel are mainly transferred to the external environment through solidified shell, ingot/mold interface and mold in turn, as shown in Figure 8.

The heat transfer resistance of each section changes continuously with time. In different stages of the steel ingot solidification process, the restrictive step of heat transfer changes

with time. In order to control the solidification process of ingots, it is extremely important to identify the restrictive steps at different stages of steel ingot solidification with different casting parameters. In the section, the heat transfer during solidification of 18-ton ingot with a large ratio of height to diameter was studied. Then, the thermal resistance of each heat transfer section in different solidification stages was found out.

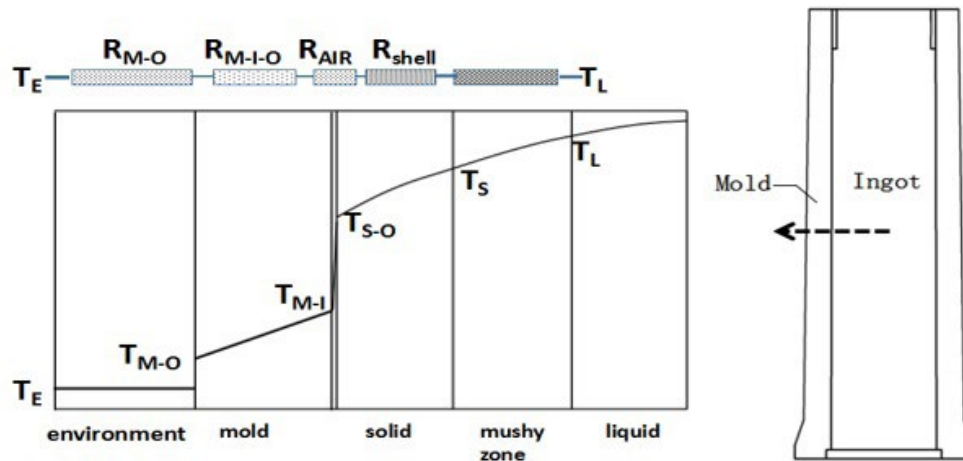


**Fig.8** - Schematic of heat transfer of steel ingot in the middle height during solidification,  $R_{M-O}$  thermal resistance of outer wall of mold;  $R_{M-I-O}$  thermal resistance of mold;  $R_{AIR}$  thermal resistance of ingot/mold interface;  $R_{SHELL}$  thermal resistance of solidified shell

In order to compare the heat transfer resistances of different heat transfer steps during solidification process, the characteristics of heat transfer in the middle height of 18-ton ste-

el ingot with large ratio of height to diameter were studied. Based on the concept of thermal resistance [ ], the thermal resistance of each heat transfer section was found out.

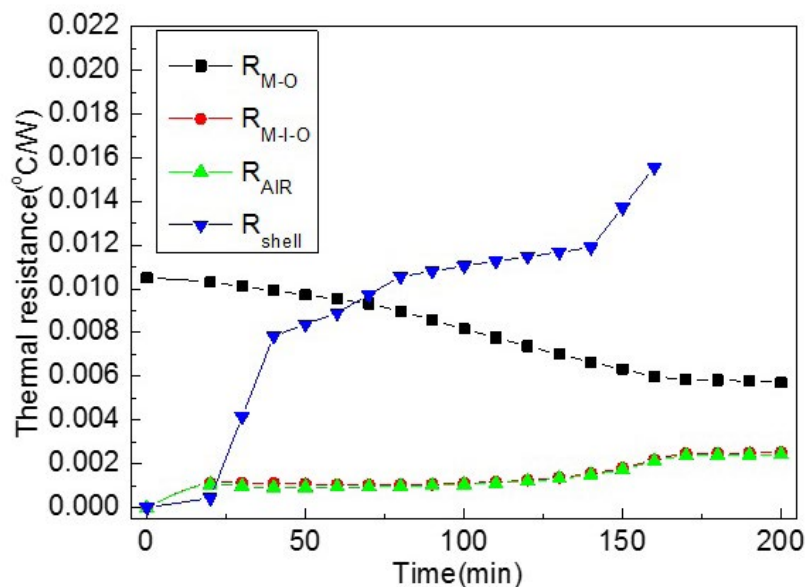


**Fig.9** - Evolutions of the transient thermal resistances of different heat transfer steps when the outer surface of the mold is cooled by air during ingot solidification

Figure 9 shows evolutions of the transient thermal resistances of different heat transfer steps when the outer wall of the mold is cooled by air during solidification of ingot. As can be seen from the figure that the thermal resistances of both the ingot/mold interface and the mold are relatively small in the whole solidification process.

Although thermal resistance of the outer wall of the mold is larger than that of other heat transfer section in the early stage of solidification, the heat transfer of the outer wall of the mold is not the restrictive step of heat transfer. At the initial stage of solidification, the heat transfer rate of the ingot is determined by both the heat transfer of ingot/mold interface and the heat storage of the mold. After the mold is filled with molten steel, the molten steel close to the mold begins to form solidified shell of a certain thickness, heat is transferred to the mold through the ingot/mold interface, which is the heat storage stage of the mold, as shown in Figure 6. At the time, the heat transfer efficiency from the outer wall of the mold to the external environment is slow, therefore, the thermal resistance of the outer wall of the mold is greater than that of other heat transfer sections. In the middle and later stages of solidification, the temperature on the outer wall of the mold is much higher, which accelerates the efficiency of heat transfer from the outer wall of the mold to the environment, the thermal resistance of the outer wall of the mold decreases gradually.

At the initial stage of solidification, the thermal resistance of solidified shell is small. With the development of solidification, then solidified shell is getting thick, which results in the increase of corresponding thermal resistance. In the middle and late stages of solidification, the thermal resistance of the solidified shell is larger than that of other heat transfer sections, especially near the final stage of solidification, the thermal resistance of solidified shell is very large, therefore the heat transfer section of the solidified shell is the restrictive step of heat transfer.

Based on the analysis of the thermal resistances of different heat transfer steps under the above condition, heat transfer of solidified shell is the main restrictive step of heat transfer in the whole solidification process for 18-ton steel ingot with large ratio of height to diameter.

### **Effect of Pouring Temperature on the Thermal Resistances**

The pouring temperature is a significant parameter in the solidification process of ingot, because it has a great influence on the defect formation of ingot such as cracks, shrinkage porosity and macrosegregation.

In order to explore the influence of different pouring temperatures on heat transfer resistances of steel ingot solidification, numerical simulations of solidification process of the 18-ton steel ingot with different pouring temperatures were carried out. Evolutions of the transient thermal resistances of different heat transfer steps with different pouring temperatures are shown in Figure 10. As can be seen from figure that at the initial stage of solidification, the change of pouring temperature has no effect on the thermal resistances of different heat transfer sections. However, in the middle and later stages of solidification, influence of variation of pouring temperature on the thermal resistance of solidified shell is obvious. Steel ingot with a high pouring temperature can lead to a small thermal resistance of solidified shell compared with that with a low pouring temperature.

It can also be seen from the Figure 10 that at early stage of solidification, the thermal resistance of the outer wall of the mold is the largest among all heat transfer sections. In the middle and late stages of solidification, the thermal resistance of the solidified shell is larger than that of other heat transfer section. In other words, the variation of pouring temperature does not change the restrictive step of heat transfer in the process of steel ingot solidification.

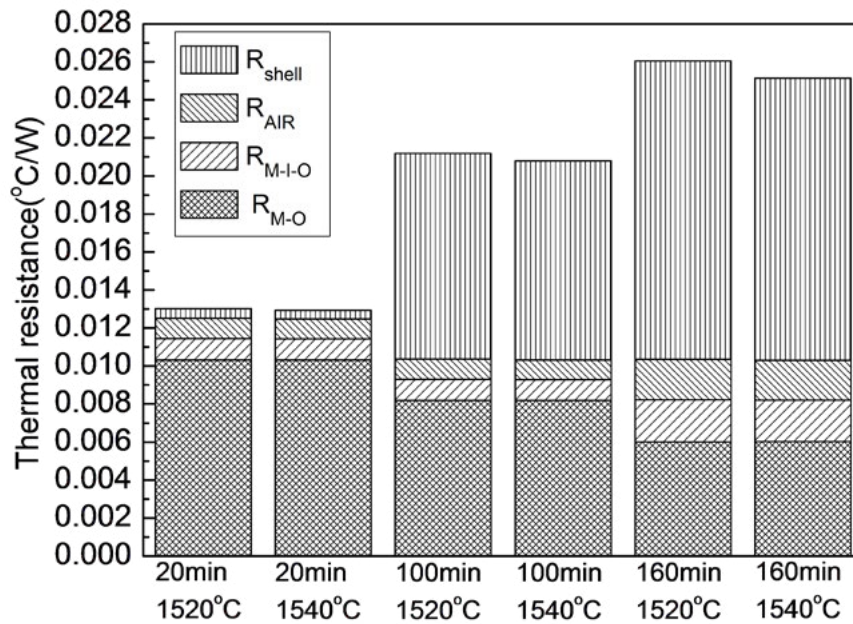


**Fig.10** - The transient thermal resistances of different heat transfer sections during steel ingot solidification with different pouring temperatures

### Conclusions

In the process of ingot solidification, the heat of molten steel is mainly transferred to the external environment through solidified shell, ingot/mold interface and mold in turn. The heat transfer step that can be controlled artificially is the heat transfer from the outer wall of the mold to the environment. Therefore, when the cooling mode of the outer wall of the mold is forced air cooling, evolutions of the transient thermal resistances of different heat transfer steps were investigated. When the outer wall of the mold is cooled by forced air, the heat transfer coefficient between the outer wall of mold and the environment is  $800\text{W}\cdot\text{m}^{-2}\cdot\text{K}^{-1}$  [21].

When the cooling mode of the outer wall of the mold is forced air cooling during solidification of ingot, evolutions of the transient thermal resistances of different heat transfer steps are shown in Figure 11. It can be seen from the figure that the thermal resistance of the solidified shell is larger than that of other heat transfer section in the whole solidification process except in the initial stage of solidification.

The thermal resistance of the solidified shell is the inherent characteristic of the ingot, which is not affected by external factors. Therefore, the solidification rate of the steel ingot is difficult to control.

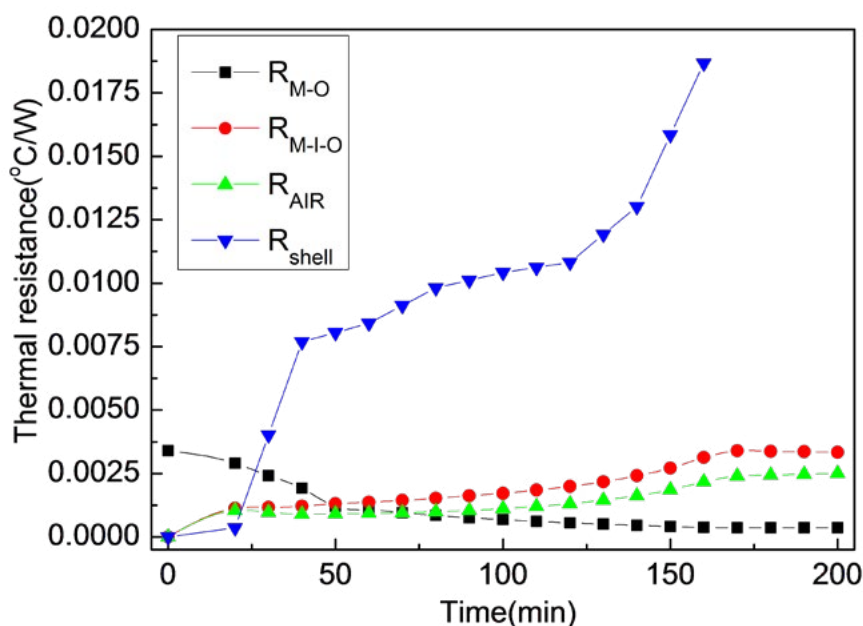


**Fig.11** - Evolutions of the transient thermal resistances of different heat transfer steps when the cooling strength of the outer surface of the mold is forced air cooling during solidification of ingot

Based on the analyses of the thermal resistances of different heat transfer steps with different casting parameters, the thermal resistances of solidified shell are still dominant in the whole solidification process for 18-ton steel ingot with large ratio of height to diameter.

### Effect of Cooling Intensity on the Thermal Resistance

Numerical simulations of solidification process of 18-ton steel ingot with a large ratio of height to diameter were investigated and the simulated results were verified by the measured temperatures and experimental sectioning investigation. The heat transfer characteristics during solidification of steel ingot with large ratio of height to diameter were dug out. The obtained results are summarized as follows:

- (1) The heat of molten steel is mainly transferred to the external environment through ingot body.
- (2) In the early stage of solidification, the thermal resistance of outer wall of mold is the largest among all heat

transfer sections. In the middle and late stages of solidification, the thermal resistance of the solidified shell is larger than that of other heat transfer sections, therefore, the heat transfer section of the solidified shell is the restrictive step of heat transfer.

(3) The variation of pouring temperature does not change the restricted heat transfer section in the process of steel ingot solidification.

(4) The outer surface of the mold is cooled by forced air can lead to that the thermal resistance of the solidified shell is larger than that of other heat transfer section in the whole solidification process except in the initial stage of solidification.

(5) The heat transfer of solidified shell is the main restrictive step of heat transfer in the whole solidification process for 18-ton steel ingot with large ratio of height to diameter.

### REFERENCES

- [1] C. Liu, Aeron. Manuf. Technol, The role and prospect of modeling and simulation in equipment manufacturing, Aeron. Manuf. Technol. 3(2008)26-29.
- [2] D. Z. Li, J. Campbell, Y.Y. Li, Filling system for investment cast Ni-base turbine blades, J Mater Procss Tech.148(2014)310-316.
- [3] B. H. Hu, K. K.Tong , X. P. Niu , Design and optimization of runner and gating systems for the die casting of thin-walled magnesium telecommunication parts through numerical simulation, J Mater. Procss Tech. 105(2000)128-133.
- [4] M.Heidarzadeh, H.Keshmiri, Influence of mould and insulation design on soundness of tool steel ingot by numerical simulation, J Iron Steel Res. Int. 20(2013)78-83.
- [5] Z. Radovic, M. Lalovic, Numerical simulation of steel ingot solidification process, J Mater Procss Tech. 160(2005)156-159.
- [6] C.J. Zhang, Y.P. Bao, M. Wang, Influence of cooling condition on solidification of large steel ingot, Metall Ital. 1 (2016)37-44.
- [7] J. Wang, P. Fu, H. Liu, D.Z. L, Shrinkage porosity criteria and optimized design of a 100-ton 30Cr 2Ni4MoV forging ingot, Mater.Design, 35(2012)446-456.
- [8] M. C. Flemings, G. E. Nereo, Macroseggregation: Part I, Trans. Mater. AIME, 239(1967)1449-1461.
- [9] M. C. Flemings, R. Mehrabian, G. E. Nereo, Macroseggregation: Part II, Trans. Mater. AIME, 242(1968)41-49.
- [10] M. C. Flemings, G. E. Nereo, Macroseggregation: Part III, Trans. Mater. AIME, 242(1968)50-55.
- [11] R.Mehrabian, M. Keane, Interdendritic fluid flow and macroseggregation; influence of gravity, Metal Mater Trans, 5 (1970)1209-1220.
- [12] W. S.Li, H. F. Shen, B. C. Liu, Three-dimensional Simulation of Thermosolutal Convection and Macroseggregation in Steel Ingots, Steel Res. Int. 81(2010)994 -1000.
- [13] W. S.Li, H.F. Shen, B.C. Liu, Numerical simulation of macroseggregation in steel ingots using a two-phase model, Int J Min Met. Mater, 19(2012)787-794.
- [14] W.Tu ,Z.Duan , B.Shen ,Three-dimensional simulation of macroseggregation in a 36-ton steel ingot using a multicomponent multiphase model, JOM. 68(2016)3116-3125.
- [15] M.Wu, A. Ludwig, A. Kharicha, A four phase model for the macroseggregation and shrinkage cavity during solidification of steel ingot ,Appl Mathe Model.41 (2016)102-120.
- [16] K. Ho, R. D. Pehlke, Mathematical modeling of porosity formation in solidification, Mater Metall Mater.Trans.B.16(1985)359-366.
- [17] Nishida. Y, Droste. W, Engler. S,The air-gap formation at the casting-mold interface and the heat transfer mechanism through the gap, Metall Mater.Trans.B, 17(1986)833-844.
- [18] P. Lan, J. Q. Zhang, Numerical analysis of interfacial heat transfer coefficient during large steel ingot solidification, J. Iron Steel Res.26(2014)29-36.
- [19] Z. Liu, Y. Zhao, Y. Zhang, Prediction of temperature distribution and porosity and shrinkage cavity formation during solidification of large steel ingots, J. Iron Steel Res. (People's Republic of China) 5 (1993)23-32.
- [20] C.J.Zhang, Y.P. Bao, Study of effective transient thermal resistances of different heat transfer sections during solidification of steel ingot, Steel Res. Int. 88(2017)1-9.
- [21] X. G.Ai, S. L. Li , N.Lv, Solidification simulation of huge rectangular ingot by different intensive cooling,Adv. Mater. Res.295(2011) 685-688.